

RAT 🐭 : Bridging RNN Efficiency and Attention Accuracy in Language Modeling

Xiuying Wei^{1*}, Anunay Yadav¹, Razvan Pascanu², Caglar Gulcehre¹
¹CLAIRE, EPFL ²Google DeepMind

Abstract

Transformers have become the cornerstone of modern large-scale language models; however, their dependence on softmax attention poses a major computational bottleneck, particularly in long-context settings. In this work, rather than following prevalent approaches such as linear attention (or SSMs) and local attention, we introduce an intermediate design called RAT between recurrence and attention mechanisms. It partitions the input into chunks, applies a simple linear recurrence within each chunk to capture local dependencies, and then performs softmax attention across chunks to model long-range interactions. By adjusting the size of the chunk, RAT enables flexible trade-offs, combining the strengths of RNN and attention. Empirically, with a chunk size of 16, the RAT layer achieves a $7\times$ improvement in training speed with 100K token sequences and $9\times$ in generation at 4K sequence length, while maintaining similar or sometimes even better accuracy compared to standard attention. We demonstrate this by training 1.3B parameter models from scratch and performing large-scale evaluations, including short- and long-context benchmarks, as well as supervised fine-tuning (SFT). We further propose a hybrid architecture that interleaves RAT with local attention. By combining efficient long-range modeling with strong local interactions, this hybrid design not only improves inference speed and reduces cache memory usage compared to attention, but also consistently enhances performance, for example, achieving an average 1 point gain in commonsense reasoning tasks, up to 4 points on code tasks, and a 1 point Rouge-L increase in a summarization SFT task. Code is available at <https://github.com/CLAIRE-Labo/RAT>.

1 Introduction

Language modeling has long been dominated by Transformer-based architectures because of their remarkable performance across a wide range of tasks. However, their reliance on full self-attention leads to quadratic complexity with respect to sequence length, which limits scalability in long-context processing. This has motivated many efforts to design more efficient attention mechanisms. Some approaches focus on local attention [1–3], and use sparse attention or recurrence to capture long-range information. Another line of work investigates the duality between linear RNNs and attention [4–7], by enforcing strict linearity constraints and introducing the notion of state expansion, which represents recurrent states as matrices rather than vectors, and shifting from per-dimension to per-head gating.

In contrast to them, we propose an alternative architecture. We argue that overusing attention in short-range contexts underutilizes its strengths and that such local processing can instead be handled more efficiently by lightweight structures such as recurrences. Based on this insight, we explore a design that lies between RNNs and attention. This design also avoids strict linearity assumptions on either side and adopts the classical recurrence form with per-dimension gating and no state expansion.

*Correspondence to xiuying.wei@epfl.ch.

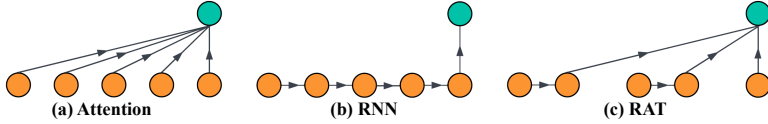


Figure 1: **Comparison of three architectures:** The circles represent the token representations and the arrows indicate the information flow for the 5th token. (a) Attention: Each token retains its representation and has full access to all previous tokens. (b) RNN: The information is progressively compressed along the sequence, and the current token only accesses the last hidden state. (c) RAT ($L=2$): Intra-chunk recurrence compresses local information, while inter-chunk attention allows direct access to previous chunks. Note that (a) and (b) can be viewed as special cases of RAT with $L = 1$ and $L = T$, respectively.

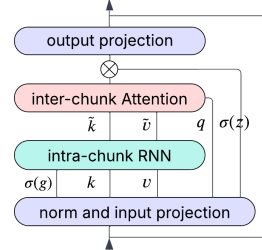


Figure 2: RAT structure. The symbol $\sigma(\cdot)$ further applies a sigmoid function to the gates. Note that we do not use extra convolution or normalization in our design.

We propose a RAT layer, which is a simple but effective temporal mixing mechanism. We divide long sequences into chunks: within each chunk, we apply recurrence for local modeling, and use softmax-based attention across chunks to access distant information directly (see Fig. 1). Recurrence efficiently captures short-range dependencies without suffering from the memory degradation issues common in long sequences, while attention over chunk-level representations enables long-range retrieval. Adjusting the size of the fragment L , RAT interpolates between attention (when $L = 1$) and RNN (when $L = T$). To make training more efficient, we adopt a lightweight gated linear recurrence [8]. We further explore a hybrid design that interleaves RAT with sliding-window attention layers [1], allowing the two mechanisms to complement each other while remaining efficient.

In terms of efficiency, our implementation relies solely on PyTorch high-level operators without any custom CUDA kernels, yet already achieves a substantial speed-up. With a chunk size of $L = 16$, the single layer latency to generate the token at position 4096 is up to $9\times$ faster than that of vanilla attention. And as shown in Table 1, the maximum throughput of the full model improves by up to $10\times$ over attention, and interleaving with local attention can also yield a $4\times$ gain.

We pretrained models with different chunk sizes at the 1.3B scale using a 4K context length, and found their perplexity (PPL) falls between that of RNNs and attention. We then evaluated them in three settings: (1) zero-shot commonsense reasoning with short contexts, (2) long-context understanding on LongBench [9], and (3) SFT on two question answering (QA) and two summarization tasks. RAT with $L = 16$ performs comparably to attention on most benchmarks and even surpasses it on some LongBench tasks. When interleaved with local attention, it achieves the strongest overall results across all variants while maintaining high efficiency. Our main contributions are as follows:

1. We propose the RAT layer as an intermediate design between RNN and attention for temporal mixing. We explore its detailed design and efficient implementation across three key scenarios, and observe significant speed.
2. We pretrain models at the 1.3B scale and evaluate them on 6 short-context, 14 long-context, and 4 SFT tasks, showing that RAT ($L=16$) performs competitively with attention.
3. We further investigate a hybrid variant that interleaves RAT with sliding-window attention, which yields the best overall performance—for example, +1 accuracy on commonsense reasoning tasks, +4 on code completion, +4 on a challenging QA SFT task, and +1 on a challenging summarization task—compared to full attention or its local variant.

Table 1: Representative results for 1.3B models across pretraining, direct evaluation, and SFT. -SWA denotes interleaving with sliding-window attention (SWA) (window size 1024). Maximum throughput is measured by generating 1024 tokens given a prompt of 3072 tokens on a H100 GPU in GH200 system. See Sec. 3 for details.

Model	Throughput token/sec	Pretrain	Direct Evaluation				SFT	
		Val. PPL	CSR Avg. acc	SQA Avg. F1	Summ Avg. Rouge-L	Code Avg. EditSum	NQA ¹ F1	QMSum Rouge-L
Attention	3052	7.61	<u>56.7</u>	18.2	<u>19.5</u>	<u>23.9</u>	61.3	<u>23.4</u>
RAT ($L=16$)	31170	7.67	55.6	19.6	20.2	17.4	60.8	23.3
Attention-SWA	4605	<u>7.61</u>	56.4	17.4	19.4	21.7	63.3	<u>23.4</u>
RAT ($L=16$) -SWA	13582	7.57	57.8	<u>18.8</u>	<u>19.5</u>	28.2	<u>63.2</u>	24.6

2 Method

2.1 Attention in temporal mixing

In softmax attention mechanisms, each token has access to all preceding tokens through a learned token-specific weighted aggregation:

$$\mathbf{y}_t = f(\mathbf{q}_t \mathbf{K}_:^\top) \mathbf{V}_: \quad (1)$$

$f(\cdot)$ denotes causal masking and the softmax function, and $f(\mathbf{q}_t \mathbf{K}_:^\top)$ are the attention weights used to aggregate $\mathbf{V}_:$. We use Python-style indexing in $\mathbf{K}_:^\top, \mathbf{V}_:$ to highlight that each query is concerned with all keys and values. Although attention is widely considered a crucial component in state-of-the-art architectures for sequence modeling, its full-token access incurs a computational complexity of $\mathcal{O}(T^2)$, where T is the length of the sequence. This quadratic growth in FLOPs can lead to substantial inefficiency during training and inference. We view attention as a **slow but lossless** module in the mixing of information between tokens and aims to combine it with a **fast but lossy** component.

2.2 Recurrence in temporal mixing

RNNs exploit sequential dependencies in the data [10, 11]. As the model processes the sequence, it maintains a summary of past information in its hidden state, allowing each step to be computed solely from the previous state and the current input. This enables efficient inference and low FLOPs, in contrast to the full-sequence access required by attention. To further improve training efficiency, recent work has explored linear RNN variants [12, 13]. For simplicity, we adopt the design proposed in Feng et al. [8], which is similar to that in Smith et al. [14]. Using diagonal matrices and removing nonlinearities, the recurrence reduces to an EMA-like gating behavior, which can be efficiently implemented with the parallel scan algorithm [14]:

$$\begin{aligned} \tilde{\mathbf{v}}_t &= \mathbf{g}_t \odot \tilde{\mathbf{v}}_{t-1} + (1 - \mathbf{g}_t) \odot \mathbf{v}_t, \\ \mathbf{y}_t &= \mathbf{z}_t \odot \tilde{\mathbf{v}}_t, \end{aligned} \quad (2)$$

where \mathbf{g}_t and $\mathbf{z}_t \in \mathbb{R}^D$ denote the forget and output gates, respectively, computed via linear projections of the input followed by a sigmoid activation. Here, D refers to the dimension of the model.

We find this simple design sufficient to achieve strong performance for short sequences. However, compressing the entire history to the current state, even with more complex recurrences, can lead to memory degradation over time [15]. As a result, RNN may struggle to retain information from distant time steps, which poses challenges for long-context tasks. Thus, in this paper, we place RNN as the **fast yet lossy** token mixing module.

2.3 RAT: a design between RNN and attention

Motivated by the complementary strengths of RNN and attention, we propose an intermediate design that combines their advantages: the speed of RNN and the global access of attention. Since RNN are effective for short sequences, while attention excels at modeling long-range dependencies, we reinterpret the input as a sequence of shorter chunks of sequences. A recurrent module is applied within each chunk to capture local dependencies, followed by cross-chunk attention to model global interactions efficiently, as shown in Fig. 1.

We divide a sequence of length T into C chunks of length L , such that $T = C \cdot L$. A token originally at position t is re-indexed as (c, l) , where c denotes the chunk index and l the position within the chunk. Within each chunk, a forget gate $\mathbf{g}_{c,l}$ is used to recurrently aggregate the value $\mathbf{v}_{c,l}$ and key $\mathbf{k}_{c,l}$ vectors, yielding updated representations $\tilde{\mathbf{v}}_{c,l}$ and $\tilde{\mathbf{k}}_{c,l}$. For each query $\mathbf{q}_{c,l}$, we compute attention on the final key vectors $\tilde{\mathbf{K}}_{:, -1}$ from all preceding chunks, as well as the current chunk’s key $\tilde{\mathbf{k}}_{c,l}$. The causal masking function $f(\cdot)$ restricts attention to the chunks before it, followed by a softmax operation. Finally, an output gate is applied to produce the output:

$$\begin{aligned}
\tilde{v}_{c,l} &= g_{c,l} \odot \tilde{v}_{c,l-1} + (1 - g_{c,l}) \odot v_{c,l} && \text{(Intra-chunk RNN)} \\
\tilde{k}_{c,l} &= g_{c,l} \odot \tilde{k}_{c,l-1} + (1 - g_{c,l}) \odot k_{c,l} && \text{(Intra-chunk RNN)} \\
y_{c,l} &= f([q_{c,l} \tilde{K}_{:, -1}^\top; q_{c,l} \tilde{k}_{c,l}^\top][\tilde{V}_{:, -1}; \tilde{v}_{c,l}]) && \text{(Inter-chunk attention)} \\
y_{c,l} &= z_{c,l} \odot y_{c,l}
\end{aligned} \tag{3}$$

The overall computation flow is illustrated in Fig. 2. Benefiting from the short length of each chunk, the RNN is both effective and computationally efficient, since its hidden state has sufficient capacity to encode short-range context without discarding much information. The attention applied across chunks then enables access to distant positions without requiring compression. As a result, the overall design preserves accuracy comparable to that of full softmax attention, while reducing computational cost, as inter-chunk attention operates over shorter contexts, with attention length inversely proportional to the chunk size.

We position this design as an **intermediate architecture** design between RNN and attention, aiming to combine their respective strengths, and refer to it as RAT. By adjusting the size of the chunk L , RAT interpolates between the RNN and the attention behaviors: when $L = T$, the model reduces to an RNN, since the entire sequence is treated as a single chunk; when $L = 1$, it resembles the attention, since each token resides in its chunk. We also explored a reversed variant that applies attention within chunks and recurrence across chunks. Although this design also allows interpolation, it underperforms RAT with equal FLOPs, likely due to suboptimal allocation of computation to local attention. Further discussion is provided in Appendix C. In the following two paragraphs, we discuss the detailed design choices for RAT.

Parameter allocation We aim to match the parameter budget of RNN and attention. In addition to the projection of the output, which introduces the parameters D^2 in all three mechanisms, both attention and RNN use additional parameters $3D^2$. These correspond to projections for the query, key, and value in attention, and for the value, the forget gate, and the output gate in RNN. To maintain the exact total parameter count for RAT, which combines both mechanisms, we adopt lightweight designs. Specifically, we consider using low-rank projections for the gates g and z , or sharing query and key projections across heads. Empirical results in Subsec. 3.3 show that sharing query q and key k typically improves performance by enabling more efficient parameter allocation. Importantly, this design does not reduce to single-head attention because the forget gate operates at a per-dimension level and introduces different elements into the gated key \tilde{k} used for the inter-chunk attention.

Positional encoding We examine how to encode positional information in RAT. Although RNN captures position through its sequential structure, the attention is usually based on explicit encodings such as RoPE [16]. For RAT, we find that applying RoPE based on chunk indices rather than original token positions yields slightly better performance, and we use cross-chunk RoPE by default, as it may better align with inter-chunk attention. See Subsec. C.2 for a more detailed discussion, including exploration of the NoPE [17] encoding.

2.4 Efficiency

We discuss the efficient implementation of RAT for the three main scenarios in language modeling, and provide pseudocode for training or prefilling in Listing 1 and for generation in Listing 2.

Training or prefilling In this setting, a sequence of tokens is processed in parallel, requiring the model to support efficient parallel computation. For the intra-chunk recurrent component in Eq. (3), we use PyTorch’s higher order operator *associative scan* to implement forward and backward passes with $\mathcal{O}(T)$ FLOPs. Compared to RNN, RAT applies the recurrent operation to both key and value representations, but chunking can reduce the scan depth from $\mathcal{O}(\log T)$ to $\mathcal{O}(\log L)$ and increase parallelism. In principle, if the chunk size L is sufficiently small, even non-linear RNNs could be viable in terms of efficiency, which we leave for future work. For inter-chunk attention, each token also attends to its own chunk’s key and value, which vary due to causal masking. To handle this efficiently, we adopt an online softmax formulation [18]: we separately compute $f(q_{c,l} \tilde{K}_{:, -1}^\top) \tilde{V}_{:, -1}$ and $f(q_{c,l} \tilde{k}_{c,l}^\top) \tilde{v}_{c,l}$, then combine them by adjusting the softmax denominator. The first term is computed

efficiently and in parallel using PyTorch’s *flex attention*, which supports custom causal masks and returns the softmax normalization term. The second term is implemented via a simple einsum.

Generation In this setting, tokens are generated sequentially. The intra-chunk recurrent component can be implemented directly using the recurrence equation, as it only requires a single-step update and does not rely on parallel operators. For inter-chunk attention, standard implementations like *flash attention* [19] can be used without any modification, since no complex causal masking is required in the generation case.

In summary, the FLOPs per token of RAT is $\mathcal{O}(C \cdot D)$, compared to $\mathcal{O}(D)$ for RNN and $\mathcal{O}(T \cdot D)$ for full attention, where C is the number of chunks, D the model dimension and T the sequence length. Notably, our current implementation achieves significant speed-ups in both training and generation without relying on custom CUDA or Triton kernels, though such kernels could further improve performance. Parallelism is particularly important for models with more than 7B parameters. We believe that RAT is compatible with both tensor and context parallelism. In particular, using a chunk size larger than 16 may reduce the communication overhead of ring-style attention in context parallelism.

3 Experiments

In this section, we present the efficiency (training, prefilling, and generation) and precision (pretraining, evaluation, and SFT) of different models. We focus primarily on the 1.3B model scale with a 4K context window, while additional discussions, including length generalization, 16K context window training, and more evaluation results, are presented in Appendix C.

3.1 Setup

For brevity, we summarize the setup of the 1.3B model with the 4K context window, which is used in most of our experiments, and provide full details in Appendix A.

Model. We adopt a Transformer architecture that interleaves a token mixing block with a hidden-state mixing block (FFN), each wrapped with residual connections and LayerNorm. We compare variants using different token mixing modules, including RNN, attention, and RAT. Inspired by recent designs that alternate global and sliding-window attention (SWA), we also explore hybrid models. Specifically, Attention-SWA alternates standard attention with SWA (window size 1024) every two layers, while RAT-SWA replaces global attention with RAT.

Efficiency We benchmark the latency of a single token mixing block, including input and output projections, on the single H100 in the GH200 system with 120GB of memory. For training and prefilling, we report the latency of processing the entire sequence. For generation, which is often the most time-consuming case, we report the latency of generating a batch of tokens at a given position. To ensure a fair comparison with strong baselines, we use *flash attention* for the attention module and the *associative scan* operator for RNN. For RAT, we follow our method design as described above. All models are wrapped with *torch.compile* and evaluated in bfloat16 using *torch.cuda.amp*.

Accuracy We pretrain the 1.3B models on a 100B token subset of the FineWeb-Edu dataset [20]. We use a learning rate of $8.0e-4$, decayed to $1.0e-6$ using cosine annealing, and a global batch size of 2M tokens. Hyperparameters are determined by DeepSeek’s attention-optimized guidelines [21] and are shared across all model variants for fair comparison. Then, we further evaluate our models using two types of benchmarks. The first is a suite of classical commonsense reasoning tasks [22] which are commonly used to assess the reasoning ability of pre-trained models in short contexts. The second is a set of English tasks from LongBench [9], where the average input length for nearly every task exceeds 4,000 tokens, and some tasks have average lengths over 10,000 tokens. LongBench tasks often include specific prompts and instructions, which pretrained-only models struggle to follow reliably. To better assess the model capability, we also compare different architectures after SFT. Specifically, we choose NarrativeQA [23] with two modes, QMSum [24], and WikiSum [25], which vary in sequence length and remain close to the pretraining domain.

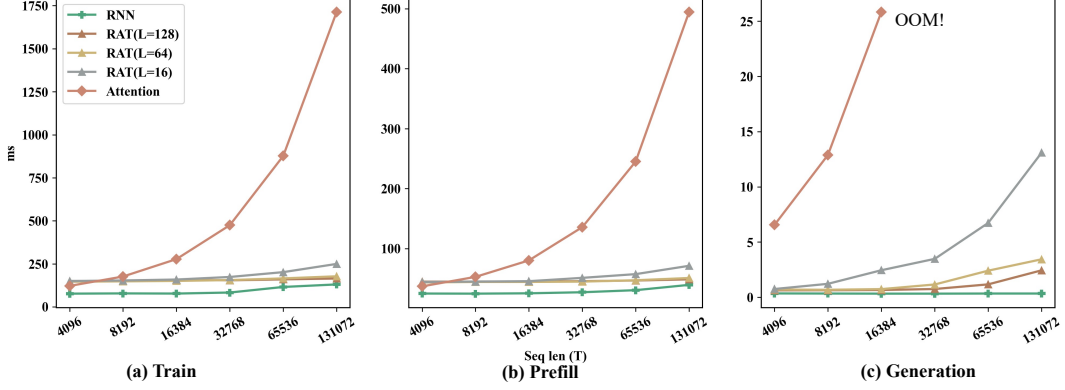


Figure 3: **Latency results.** Latency of a single RNN, RAT, or attention layer (including input and output projections) with model dimension of 2048 under (a) training, (b) prefilling, and (c) generation. (a,b) report full-sequence latency on 200K tokens; (c) reports latency for generating 512 tokens at a fixed position. RAT also reduces KV cache usage, lowering OOM risk. See Appendix B for more results.

3.2 Efficiency study

Fig. 3 presents the efficiency comparison of RNN, RAT, and attention across three scenarios: training, prefilling, and generation. For training and prefilling, when the sequence length is short (e.g., 4096), RAT is slightly slower than attention due to under-utilized GPU parallelism in the *flex attention* component (with only 256 chunks) and the overhead of *associative scan*. We believe this can be improved with better CUDA kernel optimization. As the sequence length increases, RAT becomes more efficient: for $L = 16$, we observe about $2\times$ speedup at 16K, $3\times$ at 32K, $4\times$ at 64K, and $7\times$ at 100K tokens. Additional results in Subsec. B.1 show up to $9\text{--}10\times$ at 200K. While RNN slows down beyond 32K, RAT benefits from increased intra-chunk parallelism and retains an advantage over attention. For generations, RAT($L=16$) achieves $9\times$ speedup at position 4K and around $10\times$ for longer sequences. It also reduces the usage of the KV cache, making it much less prone to OOM. RAT($L=64$) can be up to $4\times$ faster than $L = 16$ with larger batch sizes or longer inputs.

3.3 Ablation study

We conduct the ablation study on a 200M-parameter model trained on the book dataset. Allocating more parameters to the intra-chunk RNN gates yields significantly better performance than assigning them to the inter-chunk attention query and key projections, improving the perplexity by 0.4–0.5. Further replacing the original RoPE with a cross-chunk variant, where positions are indexed by chunk index, brings additional improvement, especially at long sequence lengths, with a 0.3 drop in PPL observed.

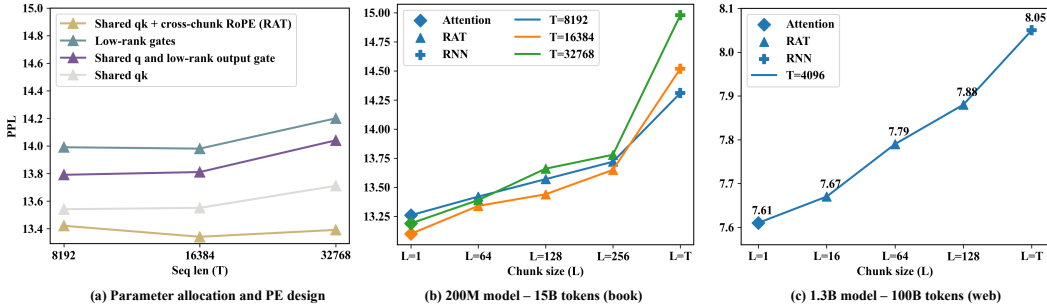


Figure 4: (a) Ablation study on RAT($L=64$). (b) and (c) show pretraining results on 200M and 1.3B models, respectively. RAT lies between RNN and attention in terms of pretraining perplexity.

3.4 Pretraining

We begin our study by examining pretraining perplexity as a foundational measure of architectural performance, showing that RAT lies between attention and RNN. The main results are presented in Fig. 4(b) and (c). In (b), on a 200M model, increasing the size of the chunk leads to higher perplexity. Viewing attention as $L = 1$ and RNN as $L = T$, we observe perplexities of 13.26 for attention, 13.42 for RAT ($L=64$), 13.72 for RAT ($L=256$), and 14.31 for RNN. Interestingly, increasing the training context from $T = 8192$ to $T = 32768$ causes a sharp increase in perplexity for RNN, while attention and RAT remain stable. Note that on a 200M model, the PPL may not decrease steadily when going to longer sequences. We then scale up to a 1.3B model trained on web data, which primarily consists of short sequences (often under 2K tokens) concatenated with separator tokens to construct 4K-length contexts. In this regime, we find that the chunk length should be reduced to 16 to match the performance of attention. Once again, increasing the size of the chunks and thus reducing the FLOPs leads to higher perplexity, strengthening the trade-off and intermediate nature of RAT.

3.5 Downstream evaluation

Table 2: We evaluate our model on six commonsense reasoning tasks using the *lm-evaluation-harness* [22]. These tasks have very short contexts, with each sample containing no more than 300 tokens. Normalized accuracy is reported when available, except for WinoGrande and LAMBADA, which use standard accuracy.

Model	ARC-C	ARC-E	HellaSwag	LAMBADA	PIQA	WinoGrande	Avg.
RNN	38.57	66.46	55.95	39.74	72.69	53.99	54.57
RAT ($L=16$)	<u>39.33</u>	67.80	56.44	44.40	72.69	53.20	55.64
Attention	37.71	66.67	<u>57.44</u>	47.84	<u>72.91</u>	57.70	<u>56.71</u>
Attention-SWA	37.20	66.20	57.09	<u>47.97</u>	72.74	<u>56.91</u>	56.35
RAT ($L=16$) - SWA	40.78	68.22	57.85	49.33	73.94	<u>56.91</u>	57.84

Commonsense reasoning The performance gap between RNN and attention is small on short and relatively simple commonsense reasoning tasks, typically within two points on average. This suggests that RNN can be surprisingly competitive in short-context settings. RAT ($L=16$) consistently outperforms RNN in most tasks, with particularly strong gains on LAMBADA, highlighting its advantage in modeling token dependencies. However, it performs poorly on WinoGrande compared to attention. One possible explanation is that WinoGrande relies heavily on subtle sentence-level cues and fine-grained referential resolution; moreover, the variance may also stem from the instability of the task itself. Interestingly, interleaving RAT with SWA yields a hybrid model (RAT ($L=16$) - SWA) that achieves the best overall performance in almost all tasks. This suggests a complementary architecture: using SWA for strong local attention and RAT for long-range dependencies can bring us a model that is not only more efficient but also more accurate than its dense counterpart. In addition, the hybrid version mitigates the weaknesses of RAT in WinoGrande, improving overall robustness. We do not include results from Gated DeltaNet [26], a recent state space model that also interleaves with sliding-window attention,² as their modeling paradigm and experimental setup differ substantially from ours.

LongBench We present the results of the evaluation for 14 English tasks in LongBench in Table 3. It is expected that no single model consistently dominates across all tasks, since LongBench employs heavy instruction-style prompts and the tasks span diverse domains. Evaluating pretrained-only models without any fine-tuning on these instruction-based tasks remains challenging; even in the original paper, 7B pretrained-only models perform much worse than tuned ones. Therefore, we focus on general performance trends across tasks, particularly average scores by task category and the top-2 models for each task.

First, RAT ($L=16$) and its hybrid variant RAT ($L=16$) - SWA consistently rank among the top two models in nearly all task groups. This is notable given that RAT ($L=16$) lags behind attention in pretraining perplexity and performs slightly worse in short-context commonsense reasoning.

²While our best model outperforms their best model (e.g., 49.33 vs. 48.76 on LAMBADA, 73.94 vs. 72.57 on PIQA, and 57.85 vs. 56.88 on HellaSwag), we do not include their results in our tables. Their approach follows a fundamentally different modeling paradigm—state space modeling—whereas our work focuses on an intermediate design between recurrence and attention. These differing motivations, together with discrepancies in window size (their 2048 vs. our 1024) and training protocols, make direct comparisons less meaningful.

Table 3: Evaluation results on LongBench. For each task, we highlight the top two values to illustrate general trends on instruction-based tasks. To save space, task numbering follows the original LongBench paper; the number-to-task mapping and token counts (measured with the LLaMA2 tokenizer) are provided in Subsec. C.4. Metrics: F1 for QA tasks, Rouge-L for summarization, and EditSum for code tasks. Specifically, accuracy is used for 4-1, F1 for 4-2, and Rouge-L for 4-3.

Model	Single-Document QA				Multi-Document QA				Summarization				Few-shot learning				Code Completion		
	1-1	1-2	1-3	Avg.	2-1	2-2	2-3	Avg.	3-1	3-2	3-3	Avg.	4-1	4-2	4-3	Avg.	6-1	6-2	Avg.
RNN	11.7	8.8	19.5	13.3	9.1	15.1	5.4	9.9	16.9	16.8	16.4	16.7	10.0	17.5	13.6	13.7	14.0	17.6	15.8
RAT(L=64)	<u>13.9</u>	13.0	27.0	18.0	<u>14.9</u>	16.3	4.3	11.8	18.9	17.7	19.9	18.8	17.5	19.2	15.2	17.3	16.2	19.7	18.0
RAT(L=16)	14.5	16.1	28.3	19.6	16.7	<u>18.9</u>	<u>6.3</u>	14.0	24.9	17.5	18.3	20.2	38.5	18.2	18.7	<u>25.1</u>	14.2	20.6	17.4
Attention	12.3	14.0	<u>28.2</u>	18.2	13.4	17.7	4.9	12.0	18.6	18.9	<u>21.0</u>	<u>19.5</u>	<u>39.5</u>	19.6	23.9	<u>27.7</u>	<u>21.3</u>	<u>26.5</u>	<u>23.9</u>
Attention-SWA	13.1	14.6	24.5	17.4	13.7	19.0	6.1	12.9	19.4	17.3	21.4	19.4	47.0	19.6	<u>25.1</u>	30.6	18.7	24.6	21.7
RAT(L=16)-SWA	12.7	<u>15.6</u>	<u>28.2</u>	<u>18.8</u>	14.2	18.1	7.4	<u>13.2</u>	<u>20.1</u>	<u>18.6</u>	19.8	<u>19.5</u>	33.5	18.4	25.6	25.8	26.3	30.1	28.2

We hypothesize that its advantage on LongBench stems from structural adaptation to very long sequences—for instance, achieving 24.9 on GovReport (3-1) (vs. 18.6 for the attention baseline) and 16.7 on HotpotQA (2-1) (vs. 13.4). Second, unlike the small gap (2 points) between RNN and attention on short-context tasks, the difference becomes much larger on LongBench, reaching up to 8 points on code completion. Finally, we note some outliers: RAT-based models underperform on TREC (4-1), a few-shot QA task evaluated via classification accuracy, for reasons not yet fully understood. In addition, RAT(L=16) performs poorly on code completion. However, its hybrid variant RAT(L=16)-SWA significantly improves in this setting, outperforming the second-best model by more than four points, consistent with earlier observations on commonsense reasoning tasks.

3.6 Supervised Fine-tuning

Since LongBench tasks are instruction-based and pretrained-only models often struggle to follow specific prompts, we further assess the performance of SFT on the QA and summarization tasks in the long-context setting, as shown in Table 4.

For NarrativeQA, where passages are extremely long and may not contain the answer within the truncated 4K-token context, we evaluate two settings: (1) summary-only, which uses only the passage summary; and (2) summary+passage, which concatenates the summary and full passage. While the latter provides more context, it also introduces much noise. In both cases, RAT(L=16)-SWA delivers strong performance while remaining efficient. Although the summary and passage contain useful information, we observe that models, particularly the attention module, perform worse in the second setting, with F1 dropping to 33. This highlights the difficulty in identifying and focusing on relevant content in noisy, extended contexts. In this setup, attention can be more easily distracted due to the absence of structural bias, which can lead to flattened attention score distributions [27]. In contrast, models based on RAT appear to be more robust, likely due to their chunk-wise structure. For summarization tasks, RNN performs better than in QA, and RAT(L=16)-SWA achieves the best result on QMSum, surpassing the next-best model by approximately 1 Rouge-L point.

Table 4: **Left:** Average and 95th percentile of context length of datasets with LLaMA2 Tokenizer. **Right:** SFT performance on long-context QA datasets with metric F1 and summarization tasks with metric Rouge-L. We consider two settings for the NarrativeQA task. NarrativeQA¹: only summary of a passage is provided. NarrativeQA²: summary plus passage is provided and the passage usually contains much irrelevant information.

Task	Avg.	95th pctl.	Model	NarrativeQA ¹	NarrativeQA ²	QMSum	WikiSum
NarrativeQA ¹	838	1296	RNN	30.5	27.4	23.2	34.3
NarrativeQA ²	97k	254k	RAT(L=16)	60.8	<u>43.5</u>	23.3	36.6
QMSum	16k	29k	Attention	61.3	33.0	23.4	36.8
WikiSum	1828	3473	Attention-SWA	63.3	39.6	23.4	<u>36.7</u>
			RAT(L=16)-SWA	<u>63.2</u>	43.7	24.6	<u>36.7</u>

4 Related work

RNN Recurrent neural networks (RNNs) have a long history of modeling sequential data [28–30], but suffer from training instabilities and lack parallelizability, especially when handling long sequences. Various approaches have been proposed to improve their trainability, such as gating mechanisms [10, 11], unitary designs [31, 32], and partially parallelizable variants [33, 34]. Moreover, RNNs face a memory bottleneck as they compress entire sequences into fixed-size hidden-state vectors. Some earlier work addressed this issue by allowing the current step to access earlier time steps directly [35–37]. For example, Koutnik et al. [36] introduces multiple timescales by updating hidden states only at predefined clock rates, while Ke et al. [37] proposes sparse, learnable connections to past tokens, with weights computed by a small MLP. More recently, state space models [38, 12, 39, 13, 40] have emerged, expanding hidden states from vectors to matrices through state expansion and reduction techniques. They also replace standard matrix multiplications with structured operations (e.g. diagonal matrices) to further enable parallel computation [14]. In contrast to these approaches, and inspired by the success of attention mechanisms, we propose integrating attention directly over the RNN history to allow explicit retrieval of past information. This design remains simple and naturally interpolates between RNN and attention behaviors. By applying inter-chunk attention to retrieve information, we avoid state expansion, which may introduce training instability and typically requires careful normalization or initialization [12, 5].

Attention While attention mechanisms have proven highly effective, they suffer from slow computation due to their full access to all previous tokens, especially in long sequences. Recently, there has been a growing interest in linear attention [4, 6, 41, 13, 5, 42, 26], which explores the dual formulation of linear RNN and linear attention. These approaches rely on strict linearity constraints and introduce state expansion and per-head gating techniques. In contrast to this duality perspective, we adopt an intermediate view between per-dimension-gated RNNs and softmax-based attention, without imposing hard linearity constraints on either side. The use of linear recurrence in our model is primarily motivated by training efficiency, but it is not strictly required at the design level. Other works have explored attention within local contexts, often motivated by the diagonal structures observed in attention maps, and have introduced recurrence or sparse attention mechanisms to provide access to earlier context [1, 2, 43, 44, 3, 45]. For example, Ma et al. [43] applies attention in chunks after gating the query and key vectors, and Behrouz et al. [3], inspired by cognitive science, focuses attention on the short-range context. In our work, we take a different approach: we use attention to model long-range dependencies, leveraging their strength in directly accessing distant tokens, while applying RNNs to short-range contexts, where they are typically less prone to memory degradation. This can also be seen as a form of attention with resolution, loosely mirroring how humans process information: short-term inputs are integrated into coherent representations, while long-term events are stored as memory anchors that can be selectively retrieved when relevant. We also find that RAT and the attention of sliding windows [1] are structurally complementary. The interleaving of the two leads to further performance improvements while being efficient.

5 Conclusion

This paper proposes the RAT structure, an intermediate architecture between RNN and attention. It segments sequences into chunks, applies RNN within each chunk to capture local dependencies, and employs attention across chunks to model long-range dependencies. We detail its architectural design and investigate its combination with the sliding-window attention mechanism. Experimental results across various settings demonstrate the efficiency and accuracy benefits of RAT, highlighting its potential for future language model development.

Limitations. Due to resource constraints and the exploratory nature of this work, our experiments are limited to models with up to 1.3B parameters. We have not yet scaled RAT to larger language models such as 7B or 14B to confirm our results hold at that scale. Additionally, we did not adopt supervised fine-tuning techniques commonly used in current industry practices, which typically involve substantial data resources and many engineering details. Instead, we followed a more classical approach based on train-test splits to evaluate performance, as our focus lies primarily on architectural design during pretraining. Lastly, RAT may still face length generalization issues from positional encoding, similar to attention. But as shown in Subsec. C.2, this can be significantly reduce by shorter inter-chunk attention spans, and we also explore the use of NoPE.

References

- [1] Iz Beltagy, Matthew E Peters, and Arman Cohan. Longformer: The long-document transformer. *arXiv preprint arXiv:2004.05150*, 2020.
- [2] Weizhe Hua, Zihang Dai, Hanxiao Liu, and Quoc Le. Transformer quality in linear time. In *International conference on machine learning*, pages 9099–9117. PMLR, 2022.
- [3] Ali Behrouz, Peilin Zhong, and Vahab Mirrokni. Titans: Learning to memorize at test time. *arXiv preprint arXiv:2501.00663*, 2024.
- [4] Angelos Katharopoulos, Apoorv Vyas, Nikolaos Pappas, and François Fleuret. Transformers are rnns: Fast autoregressive transformers with linear attention. In *International conference on machine learning*, pages 5156–5165. PMLR, 2020.
- [5] Tri Dao and Albert Gu. Transformers are ssms: Generalized models and efficient algorithms through structured state space duality. *arXiv preprint arXiv:2405.21060*, 2024.
- [6] Yutao Sun, Li Dong, Shaohan Huang, Shuming Ma, Yuqing Xia, Jilong Xue, Jianyong Wang, and Furu Wei. Retentive network: A successor to transformer for large language models. *arXiv preprint arXiv:2307.08621*, 2023.
- [7] Songlin Yang, Bailin Wang, Yikang Shen, Rameswar Panda, and Yoon Kim. Gated linear attention transformers with hardware-efficient training. *arXiv preprint arXiv:2312.06635*, 2023.
- [8] Leo Feng, Frederick Tung, Mohamed Osama Ahmed, Yoshua Bengio, and Hossein Hajimirsadeghi. Were rnns all we needed? *arXiv preprint arXiv:2410.01201*, 2024.
- [9] Yushi Bai, Xin Lv, Jiajie Zhang, Hongchang Lyu, Jiankai Tang, Zhidian Huang, Zhengxiao Du, Xiao Liu, Aohan Zeng, Lei Hou, et al. Longbench: A bilingual, multitask benchmark for long context understanding. *arXiv preprint arXiv:2308.14508*, 2023.
- [10] Junyoung Chung, Caglar Gulcehre, KyungHyun Cho, and Yoshua Bengio. Empirical evaluation of gated recurrent neural networks on sequence modeling. *arXiv preprint arXiv:1412.3555*, 2014.
- [11] S Hochreiter. Long short-term memory. *Neural Computation MIT-Press*, 1997.
- [12] Albert Gu and Tri Dao. Mamba: Linear-time sequence modeling with selective state spaces. *arXiv preprint arXiv:2312.00752*, 2023.
- [13] Antonio Orvieto, Samuel L Smith, Albert Gu, Anushan Fernando, Caglar Gulcehre, Razvan Pascanu, and Soham De. Resurrecting recurrent neural networks for long sequences. In *International Conference on Machine Learning*, pages 26670–26698. PMLR, 2023.
- [14] Jimmy TH Smith, Andrew Warrington, and Scott W Linderman. Simplified state space layers for sequence modeling. *arXiv preprint arXiv:2208.04933*, 2022.
- [15] Razvan Pascanu, Tomas Mikolov, and Yoshua Bengio. On the difficulty of training recurrent neural networks. In *International conference on machine learning*, pages 1310–1318. Pmlr, 2013.
- [16] Jianlin Su, Murtadha Ahmed, Yu Lu, Shengfeng Pan, Wen Bo, and Yunfeng Liu. Roformer: Enhanced transformer with rotary position embedding. *Neurocomputing*, 568:127063, 2024.
- [17] Amirhossein Kazemnejad, Inkit Padhi, Karthikeyan Natesan Ramamurthy, Payel Das, and Siva Reddy. The impact of positional encoding on length generalization in transformers. *Advances in Neural Information Processing Systems*, 36:24892–24928, 2023.
- [18] Maxim Milakov and Natalia Gimelshein. Online normalizer calculation for softmax. *arXiv preprint arXiv:1805.02867*, 2018.
- [19] Tri Dao, Dan Fu, Stefano Ermon, Atri Rudra, and Christopher Ré. Flashattention: Fast and memory-efficient exact attention with io-awareness. *Advances in neural information processing systems*, 35:16344–16359, 2022.

- [20] Guilherme Penedo, Hynek Kydlíček, Anton Lozhkov, Margaret Mitchell, Colin A Raffel, Leandro Von Werra, Thomas Wolf, et al. The fineweb datasets: Decanting the web for the finest text data at scale. *Advances in Neural Information Processing Systems*, 37:30811–30849, 2024.
- [21] Xiao Bi, Deli Chen, Guanting Chen, Shanhuang Chen, Damai Dai, Chengqi Deng, Honghui Ding, Kai Dong, Qiusi Du, Zhe Fu, et al. Deepseek llm: Scaling open-source language models with longtermism. *arXiv preprint arXiv:2401.02954*, 2024.
- [22] Leo Gao, Jonathan Tow, Baber Abbasi, Stella Biderman, Sid Black, Anthony DiPofi, Charles Foster, Laurence Golding, Jeffrey Hsu, Alain Le Noac’h, Haonan Li, Kyle McDonell, Niklas Muennighoff, Chris Ociepa, Jason Phang, Laria Reynolds, Hailey Schoelkopf, Aviya Skowron, Lintang Sutawika, Eric Tang, Anish Thite, Ben Wang, Kevin Wang, and Andy Zou. The language model evaluation harness, 07 2024. URL <https://zenodo.org/records/12608602>.
- [23] Tomáš Kočiský, Jonathan Schwarz, Phil Blunsom, Chris Dyer, Karl Moritz Hermann, Gábor Melis, and Edward Grefenstette. The narrativeqa reading comprehension challenge. *Transactions of the Association for Computational Linguistics*, 6:317–328, 2018.
- [24] Ming Zhong, Da Yin, Tao Yu, Ahmad Zaidi, Mutethia Mutuma, Rahul Jha, Ahmed Hassan Awadallah, Asli Celikyilmaz, Yang Liu, Xipeng Qiu, et al. Qmsum: A new benchmark for query-based multi-domain meeting summarization. *arXiv preprint arXiv:2104.05938*, 2021.
- [25] Nachshon Cohen, Oren Kalinsky, Yftah Ziser, and Alessandro Moschitti. Wikisum: Coherent summarization dataset for efficient human-evaluation. In *Proceedings of the 59th Annual Meeting of the Association for Computational Linguistics and the 11th International Joint Conference on Natural Language Processing (Volume 2: Short Papers)*, pages 212–219, 2021.
- [26] Songlin Yang, Jan Kautz, and Ali Hatamizadeh. Gated delta networks: Improving mamba2 with delta rule. *arXiv preprint arXiv:2412.06464*, 2024.
- [27] Ken M Nakanishi. Scalable-softmax is superior for attention. *arXiv preprint arXiv:2501.19399*, 2025.
- [28] Jeffrey L Elman. Finding structure in time. *Cognitive science*, 14(2):179–211, 1990.
- [29] Hava T Siegelmann and Eduardo D Sontag. On the computational power of neural nets. In *Proceedings of the fifth annual workshop on Computational learning theory*, pages 440–449, 1992.
- [30] Yoshua Bengio, Patrice Simard, and Paolo Frasconi. Learning long-term dependencies with gradient descent is difficult. *IEEE transactions on neural networks*, 5(2):157–166, 1994.
- [31] Martin Arjovsky, Amar Shah, and Yoshua Bengio. Unitary evolution recurrent neural networks. In *International conference on machine learning*, pages 1120–1128. PMLR, 2016.
- [32] Li Jing, Caglar Gulcehre, John Peurifoy, Yichen Shen, Max Tegmark, Marin Soljacic, and Yoshua Bengio. Gated orthogonal recurrent units: On learning to forget. *Neural computation*, 31(4):765–783, 2019.
- [33] James Bradbury, Stephen Merity, Caiming Xiong, and Richard Socher. Quasi-recurrent neural networks. *arXiv preprint arXiv:1611.01576*, 2016.
- [34] Tao Lei, Yu Zhang, Sida I Wang, Hui Dai, and Yoav Artzi. Simple recurrent units for highly parallelizable recurrence. *arXiv preprint arXiv:1709.02755*, 2017.
- [35] Víctor Campos, Brendan Jou, Xavier Giró-i Nieto, Jordi Torres, and Shih-Fu Chang. Skip rnn: Learning to skip state updates in recurrent neural networks. *arXiv preprint arXiv:1708.06834*, 2017.
- [36] Jan Koutník, Klaus Greff, Faustino Gomez, and Juergen Schmidhuber. A clockwork rnn. In *International conference on machine learning*, pages 1863–1871. PMLR, 2014.
- [37] Nan Rosemary Ke, Anirudh Goyal ALIAS PARTH GOYAL, Olexa Bilaniuk, Jonathan Binas, Michael C Mozer, Chris Pal, and Yoshua Bengio. Sparse attentive backtracking: Temporal credit assignment through reminding. *Advances in neural information processing systems*, 31, 2018.

- [38] Albert Gu, Karan Goel, and Christopher Ré. Efficiently modeling long sequences with structured state spaces. *arXiv preprint arXiv:2111.00396*, 2021.
- [39] Soham De, Samuel L Smith, Anushan Fernando, Aleksandar Botev, George Cristian-Muraru, Albert Gu, Ruba Haroun, Leonard Berrada, Yutian Chen, Srivatsan Srinivasan, et al. Griffin: Mixing gated linear recurrences with local attention for efficient language models. *arXiv preprint arXiv:2402.19427*, 2024.
- [40] Maximilian Beck, Korbinian Pöppel, Markus Spanring, Andreas Auer, Oleksandra Prudnikova, Michael Kopp, Günter Klambauer, Johannes Brandstetter, and Sepp Hochreiter. xlstm: Extended long short-term memory. *arXiv preprint arXiv:2405.04517*, 2024.
- [41] Bo Peng, Eric Alcaide, Quentin Anthony, Alon Albalak, Samuel Arcadinho, Stella Biderman, Huanqi Cao, Xin Cheng, Michael Chung, Matteo Grella, et al. RwkV: Reinventing rnns for the transformer era. *arXiv preprint arXiv:2305.13048*, 2023.
- [42] Songlin Yang, Bailin Wang, Yu Zhang, Yikang Shen, and Yoon Kim. Parallelizing linear transformers with the delta rule over sequence length. *arXiv preprint arXiv:2406.06484*, 2024.
- [43] Xuezhe Ma, Chunting Zhou, Xiang Kong, Junxian He, Liangke Gui, Graham Neubig, Jonathan May, and Luke Zettlemoyer. Mega: moving average equipped gated attention. *arXiv preprint arXiv:2209.10655*, 2022.
- [44] Xuezhe Ma, Xiaomeng Yang, Wenhan Xiong, Beidi Chen, Lili Yu, Hao Zhang, Jonathan May, Luke Zettlemoyer, Omer Levy, and Chunting Zhou. Megalodon: Efficient llm pretraining and inference with unlimited context length. *Advances in Neural Information Processing Systems*, 37:71831–71854, 2024.
- [45] Amirkeivan Mohtashami and Martin Jaggi. Landmark attention: Random-access infinite context length for transformers. *arXiv preprint arXiv:2305.16300*, 2023.
- [46] Jack W Rae, Anna Potapenko, Siddhant M Jayakumar, Chloe Hillier, and Timothy P Lillicrap. Compressive transformers for long-range sequence modelling. *arXiv preprint*, 2019. URL <https://arxiv.org/abs/1911.05507>.
- [47] Yonatan Bisk, Rowan Zellers, Jianfeng Gao, Yejin Choi, et al. Piqa: Reasoning about physical commonsense in natural language. In *Proceedings of the AAAI conference on artificial intelligence*, volume 34, pages 7432–7439, 2020.
- [48] Peter Clark, Isaac Cowhey, Oren Etzioni, Tushar Khot, Ashish Sabharwal, Carissa Schoenick, and Oyvind Tafjord. Think you have solved question answering? try arc, the ai2 reasoning challenge. *arXiv:1803.05457v1*, 2018.
- [49] Rowan Zellers, Ari Holtzman, Yonatan Bisk, Ali Farhadi, and Yejin Choi. Hellaswag: Can a machine really finish your sentence? *arXiv preprint arXiv:1905.07830*, 2019.
- [50] Biao Zhang and Rico Sennrich. Root mean square layer normalization. *Advances in Neural Information Processing Systems*, 32, 2019.
- [51] Team Cohere, Arash Ahmadian, Marwan Ahmed, Jay Alamm, Milad Alizadeh, Yazeed Alnumay, Sophia Althammer, Arkady Arkhangorodsky, Viraat Aryabumi, Dennis Aumiller, et al. Command a: An enterprise-ready large language model. *arXiv preprint arXiv:2504.00698*, 2025.
- [52] Bowen Peng, Jeffrey Quesnelle, Honglu Fan, and Enrico Shippole. Yarn: Efficient context window extension of large language models. *arXiv preprint arXiv:2309.00071*, 2023.
- [53] bloc97. NTK-Aware Scaled RoPE allows LLaMA models to have extended (8k+) context size without any fine-tuning and minimal perplexity degradation, 2023.
- [54] Jie Wang, Tao Ji, Yuanbin Wu, Hang Yan, Tao Gui, Qi Zhang, Xuanjing Huang, and Xiaoling Wang. Length generalization of causal transformers without position encoding. *arXiv preprint arXiv:2404.12224*, 2024.
- [55] Cheng-Ping Hsieh, Simeng Sun, Samuel Krman, Shantanu Acharya, Dima Rekeshe, Fei Jia, Yang Zhang, and Boris Ginsburg. Ruler: What’s the real context size of your long-context language models? *arXiv preprint arXiv:2404.06654*, 2024.

A Implementation details

A.1 Algorithm

We provide the pseudocode for the training and prefilling modes of RAT in Listing 1, and the pseudocode for the generation mode in Listing 2.

```
1 def merge_last_token_stable
  (inter_out, intra_out, inter_lse, intra_lse):
2   # Merge previous chunk's output and current chunk's output safely
3   # by adjusting the base of the exponential in softmax
4   max_lse = maximum(inter_lse, intra_lse)
5   inter_lse_exp = exp(inter_lse - max_lse)
6   intra_lse_exp = exp(intra_lse - max_lse)
7   denom = intra_lse_exp + inter_lse_exp
8   intra_adjust = (intra_lse_exp / denom).unsqueeze(-1)
9   inter_adjust = (inter_lse_exp / denom).unsqueeze(-1)
10  return inter_out * inter_adjust + intra_out * intra_adjust
11
12
13 def train_or_prefill
  (z, g, q, k, v, num_chunk, chunk_size, num_head, softmax_scale):
14   """
15   Args:
16   z: (B, T, D), output gate after sigmoid function
17   g: (B, T, D), forget gate after sigmoid function
18   v: (B, T, D), value vectors in attention
19   q, k: (B, T, D), shared query and key vectors in attention
20   Returns:
21   out: (B, T, D)
22   """
23   bs, seq_len, d_model = shape(z)
24   k, v = [
25     rearrange(m, "b (c l) d -> b c l d", c=num_chunk) for m in (k, v)]
26
27   # Intra-chunk RNN: apply associative scan along the "l" dimension
28   intra_v = ascan(g, (1.0 - g) * v)
29   intra_k = ascan(g, (1.0 - g) * k)
30
31   # Rearrange for multi-head attention
32   intra_v = rearrange(intra_v, "b c l (a p) -> b a (c l) p", a=num_head)
33   intra_k = rearrange(intra_k, "b c l (a p) -> b a (c l) p", a=num_head)
34   q = rearrange(q, "b t (a p) -> b a t p", a=num_head)
35
36   # Apply inter-chunk RoPE
37   q, intra_k = apply_rope(q, intra_k)
38
39   # Extract chunk's end representation for inter-chunk attention
40   chunk_intra_k = intra_k[..., chunk_size - 1::chunk_size, :]
41   chunk_intra_v = intra_v[..., chunk_size - 1::chunk_size, :]
42
43   # Inter-chunk attention using flex_attention
44   # with chunk-level causal mask and returning log-sum-exp scores
45   block_mask = create_block_mask(
46     lambda b, h, q_idx, kv_idx: q_idx // chunk_size > kv_idx,
47     1, 1, q.shape[2], num_chunk
48   )
49   inter_out, inter_lse = flex_attention(
50     q, chunk_intra_k, chunk_intra_v,
51     scale=softmax_scale,
52     block_mask=block_mask,
53     return_lse=True
54   )
```

```

54
55     # Compute logits with
56     the current chunk's k, required separately due to causal masking
57     intra_lse
58     = einsum("batp, batp -> bat", q, intra_k) * softmax_scale
59
60     # Merge outputs
61     from previous chunks and current chunk (due to causal masking)
62     out =
63         merge_last_token_stable(inter_out, intra_v, inter_lse, intra_lse)
64     out = rearrange(out, "b a t p -> b t (a p)", a=num_head)
65     return z * out

```

Listing 1: Pseudo code for the training or prefilling modes of RAT. We use Pytorch's *flex attention* and *associative scan* for implementation.

```

1 def gen(z, g, q, k, v, chunk_start, num_head, cache):
2     """
3     Args:
4         z: (B, 1, D), output gate after sigmoid
5         g: (B, 1, D), forget gate after sigmoid
6         v: (B, 1, D), value vector
7         q, k: (B, 1, D), shared query and key vectors across heads
8         chunk_start: int, index of current chunk
9         cache: tuple of four tensors
10             lastkcache
11             : (B, 1, D), last token k in current chunk (for RNN-style update)
12             lastvcache
13             : (B, 1, D), last token v in current chunk (for RNN-style update)
14             kcache: (B, A, C, P) or
15                 (B, num_head, num_chunk, head_dim): cached k at each chunk's end
16             vcache: (B, A, C, P) or
17                 (B, num_head, num_chunk, head_dim): cached v at each chunk's end
18             # Note: KVCache is stored per chunk, not per token.
19     Returns:
20         out: (B, 1, D)
21     """
22     lastkcache, lastvcache, kcache, vcache = cache
23
24     # Intra-chunk RNN: Recurrent update within the current chunk
25     intra_k = g * lastkcache + (1.0 - g) * k
26     intra_v = g * lastvcache + (1.0 - g) * v
27     lastkcache.copy_(intra_k)
28     lastvcache.copy_(intra_v)
29
30     # Rearrange input for attention
31     intra_k = rearrange(intra_k, "b t (a p) -> b a t p", a=num_head)
32     intra_v = rearrange(intra_v, "b t (a p) -> b a t p", a=num_head)
33     q = rearrange(q, "b t (a p) -> b a t p", a=num_head)
34
35     # Apply RoPE
36     q, intra_k = apply_rope(q, intra_k)
37
38     # Update the current chunk's kvcache
39     kcache[:, :, chunk_start:chunk_start + 1] = intra_k
40     vcache[:, :, chunk_start:chunk_start + 1] = intra_v
41
42     # Inter-chunk
43     attention: standard attention over cached chunk representations
44     attn_out = scaled_dot_product_attention(
45         q, kcache[:, :, :chunk_start + 1], vcache[:, :, :chunk_start + 1], is_causal=False
46     )
47     out = rearrange(out, "b a t p -> b t (a p)", a=num_head)

```

```
return z * out
```

Listing 2: Pseudo code for the generation mode of RAT. We simply use the *flash attention* (Pytorch’s one). Note that KVCache of RAT is reduced from T to C compared to the attention module.

A.2 Experiments

Dataset In our preliminary studies, we use the PG19 dataset [46], a long-form English book corpus with inherently long contexts. For the 1.3B model experiments, we adopt the FineWeb-Edu dataset [20], using its 100B-token randomly sampled version downloaded from the HuggingFace repository. To match the pretraining context length, we concatenate documents using a separator token. Note that web samples are usually very short, compared to the book dataset. For downstream evaluation, we consider a suite of classical commonsense reasoning benchmarks from the Eleuther AI evaluation harness [22], including PIQA [47], ARC-C [48], and HellaSwag [49]. In the LLaMA2 tokenizer, we observe that the inputs of these tasks typically contain fewer than 300 tokens. For the LongBench evaluation, in Table 5 we provide a mapping of task numbering to names and annotate their input lengths for each task, offering a rough indication of task difficulty with respect to input length. For SFT-based tasks, we have elaborated sequence lengths in the main text. As LongBench and SFT tasks often involve very long inputs, we apply truncation in the middle to preserve information at both the beginning and the end.

Table 5: We provide a mapping from task numbers to task names. NQA (NarrativeQA), MQA (MultiFieldQA-en), HQA (HotpotQA), WQA (2WikiMultiHopQA), MSQ (Musique), GR (GovReport), MN (MultiNews), TQA (TriviaQA), and RBP (RepoBench-P). We also report the average input length and the 95th percentile input length of each task, measured in tokens using the LLaMA2 tokenizer.

Task	Single-Document QA			Multi-Document QA			Summarization			Few-shot learning			Code Completion	
	1-1	1-2	1-3	2-1	2-2	2-3	3-1	3-2	3-3	4-1	4-2	4-3	6-1	6-2
Name	NQA	Qasper	MQA	HQA	WQA	MSQ	GR	QMSum	MN	TREC	TQA	SAMSum	LCC	RBP
Avg.	36037	5780	8115	15329	8483	18555	12280	15980	3156	7792	14098	11168	4307	14818
95th pctl.	77966	10164	14994	19755	16939	20066	25721	29069	7135	12532	25006	19823	10401	31937

200M model We start with a 200M-parameter model in our preliminary study, with a model dimension of 1024, 12 transformer layers, and head dimension of 64. The rotary position embedding (RoPE) base is set to 10,000. We use the GPT2 tokenizer. Following Mohtashami and Jaggi [45], we repeat the PG19 training split five times to reach a total of 15B training tokens. The learning rate is scheduled using cosine annealing, starting at 6.0×10^{-4} and decaying to 1.0×10^{-6} , with a warm-up ratio of 10%. We use the AdamW optimizer with a weight decay of 0.1 and $\beta = (0.9, 0.98)$. Gradient clipping is applied with a threshold of 1.0, and the global batch size is set to 1M tokens. We explore training with three different context lengths: 8K, 16K, and 32K. Training these models on 4 H100 GPUs takes approximately 5 to 14 hours. In particular, the attention model requires up to 14 hours when the sequence length is $T = 32768$, whereas the RAT (L=16) model completes training in about 7 hours under the same setting.

1.3B model The 1.3B-parameter model uses a model dimension of 2048, 24 transformer layers, and a head dimension of 128, equipped with RMSNorm [50] and without bias. The RoPE base is also set to 10,000. The model parameters are initialized using a Gaussian distribution with a standard deviation of 0.02. We adopt the LLaMA2 tokenizer in the following studies. For pretraining, we use a cosine-annealed learning rate schedule starting at 8.0×10^{-4} and decaying to 1.0×10^{-6} , with 5% warmup. The global batch size is set to 2M tokens. We primarily train with a context window of 4K tokens and include additional experiments with a 16K context window, for which the RoPE base is increased to 500,000. Each model is trained on 16 H100 GPUs, requiring approximately 2 to 3 days to complete.

For LongBench evaluation, we follow the default prompts with greedy decoding for all tasks except summarization. For summarization, we apply a repetition penalty of 1.2 to address the common issue in pretrained-only models of generating repetitive outputs under instructional prompts. For SFT tasks, we train the models on the official training splits with an answer-only loss and evaluate them on the corresponding test sets. Although we explored different hyperparameters during the early experimentation, we observed that the relative trends remained largely stable. Thus, we fix

the learning rate and batch size to $(1.0 \times 10^{-5}, 128)$ for large datasets, and $(1.0 \times 10^{-5}, 32)$ for the smaller QMSum [24] task, following common practice for 1B-scale models. The weight decay is set as 0.01, and all other hyperparameters follow the pretraining setup. We sweep over the number of epochs and report the best result for each dataset and architecture. In practice, QA tasks typically converge in 1–2 epochs, while summarization benefits from slightly longer training.

B Efficiency

B.1 Latency

To supplement Fig. 3 in main text, we put the concrete latency number of a single layer in Table 6, Table 7, and Table 8.

Table 6: Single layer (including input and output projections) training time across different sequence lengths. The latency (ms) is tested on 200K tokens.

Model	4096	8192	16384	32768	65536	131072	262144
RNN	77.00	78.42	77.50	83.50	115.83	130.62	195.30
RAT(L=128)	150.19	150.76	156.65	154.52	159.94	165.07	206.46
RAT(L=64)	146.25	148.46	151.10	155.83	165.58	177.78	227.76
RAT(L=16)	150.08	153.63	158.98	173.89	202.00	249.79	378.11
Attention	122.06	176.44	277.61	474.90	877.14	1713.82	3417.48
Attention/RAT(L=16)	$0.81\times$	$1.15\times$	$1.75\times$	$2.73\times$	$4.34\times$	$6.86\times$	$9.04\times$

Table 7: Single layer (including input and output projections) prefilling time across different sequences lengths. The latency (ms) is tested on 200K tokens.

Model	4096	8192	16384	32768	65536	131072	262144
RNN	24.93	24.75	25.32	27.09	30.54	39.40	56.16
RAT(L=128)	44.74	44.78	45.09	45.50	46.67	48.62	51.75
RAT(L=64)	43.46	44.27	44.27	44.83	47.08	50.83	57.38
RAT(L=16)	44.03	44.90	45.53	51.08	57.31	71.18	99.53
Attention	36.93	52.71	80.21	135.68	245.14	494.62	997.50
Attention/RAT(L=16)	$0.84\times$	$1.17\times$	$1.76\times$	$2.66\times$	$4.28\times$	$6.95\times$	$10.02\times$

B.2 Maximum throughput

As RAT also reduces cache memory usage, we report the maximum throughput of the full 1.3B model across different sequence lengths in Fig. 5. For example, RAT(L=16) achieves an approximately $10.2\times$ higher throughput than the baseline attention model at $T = 4096$, and improves further to $15.6\times$ at $T = 16384$. Similarly, RAT(L=16)–SWA reaches $4.5\times$, $8.0\times$, and $13.9\times$ higher throughput over attention at $T = 4096$, 8192, and 16384, respectively.

C Accuracy

C.1 Reversed design of RAT

Instead of employing recurrence within each chunk, we also explored a reversed design that applies attention inside the chunk, followed by recurrence to capture long-range dependencies. For this reversed design, standard RoPE is sufficient. However, with respect to parameter allocation, we found it crucial to retain the key vector in the attention module as a full tensor, as sharing it together with the query vector leads to a collapse into single-head attention. Thus, our final reversed design shares the query vector across attention heads, employs low-rank matrices for the projection used for output gate, and preserves full projections for both the forget gate and the key vector. Results of the reversed design are put in Table 9. It can be observed that, under identical FLOP constraints, this design

Table 8: Single layer (including input and output projections) generation time at the specified position. The latency (ms) is tested on generating batches of tokens with $B = 64$, $B = 512$, and $B = 1024$.

Model	4096	8192	16384	32768	65536	131072	262144
$B = 64$							
RNN	0.36	0.33	0.34	0.33	0.33	0.33	0.33
RAT (L=128)	0.62	0.60	0.61	0.63	0.66	0.66	0.68
RAT (L=64)	0.67	0.64	0.66	0.70	0.73	0.74	1.03
RAT (L=16)	0.62	0.65	0.64	0.68	1.04	1.82	3.42
Attention	1.15	1.73	3.33	6.66	12.94	26.8	OOM
$B = 512$							
RNN	0.35	0.34	0.33	0.33	0.34	0.34	0.33
RAT (L=128)	0.63	0.64	0.66	0.75	1.17	2.44	3.46
RAT (L=64)	0.70	0.68	0.74	1.16	2.41	3.44	6.69
RAT (L=16)	0.75	1.22	2.45	3.48	6.73	13.09	25.76
Attention	6.56	12.89	25.84	OOM	OOM	OOM	OOM
$B = 1024$							
RNN	0.36	0.36	0.35	0.35	0.35	0.36	0.35
RAT (L=128)	0.73	0.75	0.95	1.35	2.54	4.64	6.98
RAT (L=64)	0.74	0.94	1.35	2.48	4.67	7.02	13.45
RAT (L=16)	1.38	2.56	4.63	7.04	13.51	26.43	OOM
Attention	13.04	25.70	OOM	OOM	OOM	OOM	OOM

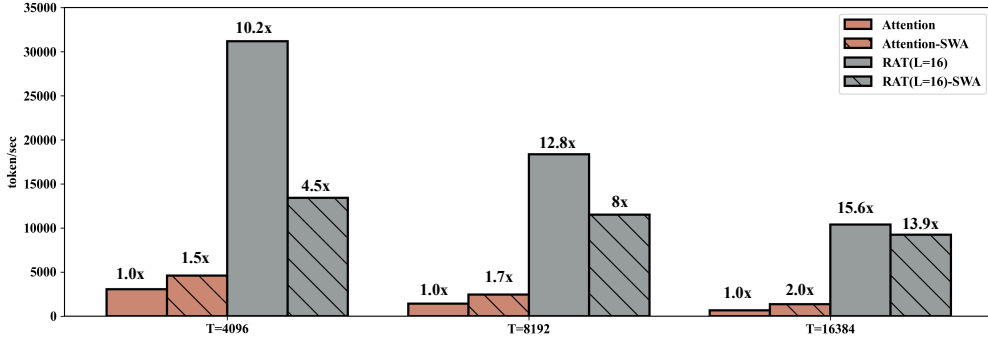


Figure 5: We measure the maximum throughput of the full 1.3B model for generating 1024 tokens under different prefilling lengths. For each total sequence length T , the prefilling length is set to $T - 1024$. For example, $T = 4096$ corresponds to a prefilling of 3072 tokens, while $T = 8192$ and $T = 16384$ correspond to 7168 and 15360 tokens, respectively. When the sequence length increases, the maximum throughput ratio between RAT and attention rises from $10.2\times$ to $15.6\times$, highlighting the strong efficiency advantage of RAT in long-context generation.

significantly underperforms RAT. For example, to match the FLOPs budget of $\mathcal{O}(T/64)$, it requires chunk sizes of 128, 256, and 512 for sequence lengths of 8192, 16384, and 32768, respectively. Most of the computational cost is spent within a small local window of 128 tokens, while excessive burden is placed on the inter-chunk recurrence, ultimately leading to high perplexity. Only when we reduce the number of chunks to 16 does the perplexity drop below 14.00. Therefore, while the reversed design also allows for interpolation between attention and RNN (reducing to attention when $L = T$, and to RNN when $L = 1$), we choose to focus on RAT due to its more efficient utilization of FLOPs.

Table 9: Perplexity results of the reversed design, where attention is applied within chunks and RNN is used across chunks. Experiments are conducted on the 200M model trained on the PG19 book dataset. Under the same FLOPs, it can be observed that RAT significantly outperforms its reversed counterpart.

Method	FLOPs	T = 8192	T = 16384	T = 32768
RAT (L=128)	$\mathcal{O}(T/128)$	13.57	13.44	13.66
RAT (L=64)	$\mathcal{O}(T/64)$	13.42	13.34	13.39
RAT-Reversed (C=128)	$\mathcal{O}(T/128)$	14.53	14.35	14.37
RAT-Reversed (C=64)	$\mathcal{O}(T/64)$	14.21	14.06	14.02
RAT-Reversed (C=16)	$\mathcal{O}(T/16)$	13.69	13.48	13.50
Attention	$\mathcal{O}(T)$	13.26	13.10	13.19

Table 10: Pretraining and downstream evaluation results of 1.3B models using either RoPE or NoPE positional encodings. RoPE is used in the main text, while NoPE is trained for investigating length extrapolation. Notably, NoPE achieves reasonable performance even at the 1B model scale with only 100B training tokens.

Method	PE	Pretrain PPL	HellaSwag acc_norm	LAMBADA acc	PIQA acc_norm
Attention-SWA	RoPE	7.61	57.1	48.0	72.7
RAT (L=16)-SWA	RoPE	7.57	57.9	49.3	73.9
Attention-SWA	NoPE	7.69	56.4	47.3	72.7
RAT (L=16)-SWA	NoPE	7.63	56.8	47.8	73.7

C.2 Length generalization

Because of the use of softmax-based attention and RoPE at the inter-chunk level, it is reasonable to expect that RAT may also face challenges in length generalization, where the model is trained on short sequences but evaluated on much longer ones. To study this, we consider SWA variants using either RoPE or NoPE for attention and RAT, following recent practices that interleave attention with local attention modules and apply positional encodings only in the local attention. This design has been adopted in practice and has shown promising results [51].

As shown in Fig. 6, the RNN performs very steadily as the test sequence length increases. However, within the training context, it has the highest loss among all models. With RoPE, both Attention-SWA and RAT (L=16)-SWA experience a sharp increase in loss when the sequence length goes beyond 6000. The increase is more severe in the attention model than in the RAT variant. This is likely because RAT reduces the effective attention span by attending only to inter-chunk positions, which may offer better robustness to extrapolation.

We also pretrain NoPE versions, where no positional encodings are used in attention or RAT layers. Interestingly, these NoPE models show reasonable performance, as reported in Table 10. While their pretraining perplexities are higher than those of the RoPE variants, the gap remains small, especially considering the 1.3B model size and 100B-token training budget. To further verify this,

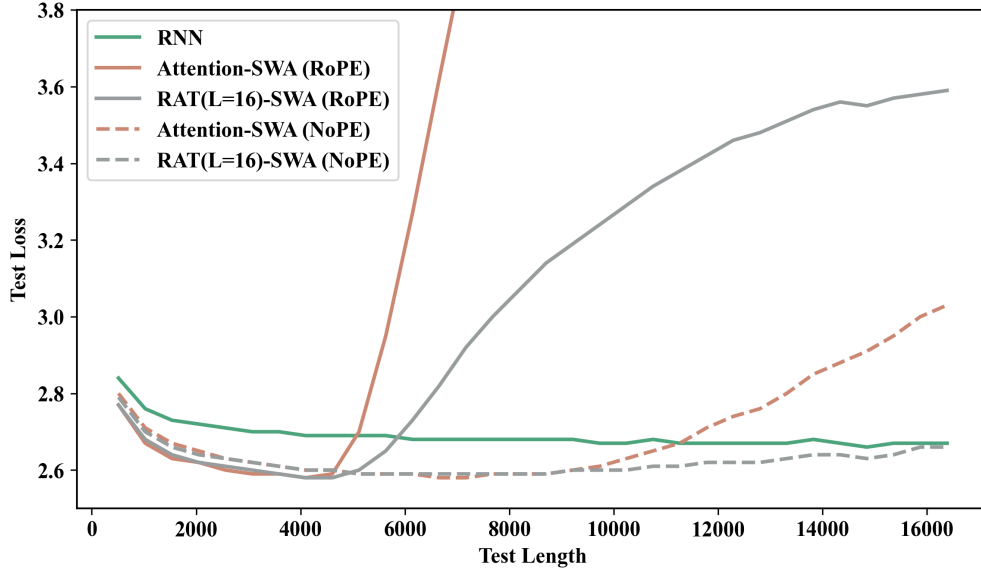


Figure 6: Evaluation at different test lengths for pretrained models trained with a 4K context window. RAT (L=16)-SWA with NoPE achieves the best overall performance, exhibiting strong generalization up to $T = 16384$ while maintaining low loss within the training context.

we evaluate the models on several commonsense reasoning tasks and obtain promising results. We expect that NoPE will perform even better with larger models and longer training. In terms of length extrapolation, using NoPE significantly improves the robustness for both Attention-SWA and RAT (L=16)–SWA. Among them, RAT (L=16)–SWA with NoPE shows the most stable performance, maintaining low loss even at a sequence length of 16,384.

In conclusion, we find that RAT can outperform the attention module in length generalization, both with RoPE and with NoPE. Still, the problem is not fully solved, as none of the models reach the stability level of the simple RNN. While many techniques have been proposed to improve length extrapolation in attention models, they should also be considered for RAT, as RAT essentially redirects attention from every position to inter-chunk locations. For example, RoPE extrapolation in the attention module can be improved using methods from Peng et al. [52], bloc97 [53], and NoPE extrapolation has been studied in Wang et al. [54], which points out that NoPE still has a context length limit, though it performs better than RoPE. Their work links the failure to shifts in attention distributions and proposes tuning the temperature of attention heads to improve extrapolation. We believe such methods could also be applied to RAT, and leave further exploration of these techniques to future work.

C.3 16K context window

Table 11: Performance of 1.3B models with a 16K context window, including pretraining perplexity, commonsense reasoning accuracy (short-context), and SFT results on long-context tasks. For SFT, we focus on tasks that still have long context even with the 16K context window, such as QMSum and NarrativeQA³. For NarrativeQA³, we adopt the passage-only setting from the original paper instead of the summary+passage setup used in NarrativeQA². Although passages are still truncated at 16K, most information are preserved, making passage-only a more meaningful and challenging evaluation setting.

Model	Throughput token/sec	Pretrain	Evaluation							SFT	
		Val.	ARC-C	ARC-E	HellaSwag	LAMBADA	PIQA	WinoGrande	Avg.	NarrativeQA ³	QMSum
RNN	130K	8.09	37.4	65.7	54.2	37.6	72.6	53.4	53.5	15.4	22.8
RAT (L=16)	10376	7.52	36.5	64.8	55.8	45.6	71.5	53.5	54.6	21.6	24.2
Attention	667	<u>7.44</u>	36.8	67.5	<u>57.0</u>	43.9	<u>73.2</u>	57.1	<u>55.9</u>	23.3	23.8
Attention-SWA	1347	7.45	<u>36.9</u>	65.8	56.6	<u>47.6</u>	72.5	55.6	55.8	20.3	23.3
RAT (L=16)–SWA	9244	7.42	38.5	67.5	57.6	47.7	73.3	<u>57.0</u>	56.9	<u>22.6</u>	24.6

We also pretrain the models with a 16K context length. However, we observe that directly pretraining with such a long context window may lead to issues, as most web data is relatively short and needs to be concatenated by the separate token to fill the window. Due to the lack of naturally long-context data, the model may fail to learn true long-context capabilities. We believe this setting would benefit from more careful strategies, such as continued pretraining and balanced long-context data sources. Nonetheless, due to resource limitations, we directly pretrain the models on a 16K context length in this work, and hope that the results can reflect the ability of different architectures to handle longer contexts to some extent.

Due to the short web data used during pretraining, we consider evaluating the models on short-context tasks, or applying SFT on long-context tasks that contain real long sequences. As shown in Table 11, overall, the performance of RAT (L=16) stays in between of RNN and attention, and RAT (L=16)–SWA performs the best. It achieves a 0.02 pretraining lower perplexity than attention, and improves by about 1 point on average in commonsense reasoning and 0.8 points on QMSum. However, it underperforms attention around 0.7 points in F1 score on the NarrativeQA³ task, unlike in the 4K context length setting. On the other hand, the maximum throughput improves significantly: from $\sim 4.5\times$ compared to attention at the 4K context window to $\sim 13.9\times$ at 16K. This suggests that, to pursue higher accuracy performance, we may consider increasing the local attention window size (e.g., from 1024 to 4096) under the 16K context length setting.

C.4 Needle-in-Haystack (retrieval ability)

To evaluate retrieval capabilities—an area where attention-based architectures are known to excel, and where RNNs typically fall short—we conduct experiments on the Needle-in-Haystack tasks. In these tasks, a “needle” (e.g., a magic number or UUID) is embedded within irrelevant passages, noisy text, or mixed with multiple key-value pairs. Each key-value pair is presented as a short identifier (the key) followed by its associated value, and the model is prompted to retrieve the correct value given a specific key.

We adopt the RULER benchmark [55] and evaluate a range of Needle-in-Haystack task configurations. Specifically, task `single_1` involves retrieving a specific number from a background filled with repeated noise. In `single_2`, the background is replaced with natural stories. `single_3` increases the difficulty by requiring retrieval of a long and complex UUID. The `multikey` tasks are more challenging than the single-key ones, as they introduce multiple such key-value pairs into the context. In particular, `multikey_2` and `multikey_3` consist almost entirely of densely packed key-value pairs, among which only a single key is queried at the end. This makes the task especially challenging, as the model must retrieve the correct item from a highly cluttered input full of distractors. And `multikey_3` further incorporates the complex UUID format. In the `multiquery` and `multivalue` settings, the model is required to resolve multiple retrieval targets—either by answering several distinct queries, or by retrieving all values associated with a single key. For detailed definitions of each task, we refer the reader to the benchmark documentation.

During evaluation, we observed that models may fail to interpret certain prompts correctly. For instance, prompts like “A special magic number is hidden within the following text. Make sure to memorize it. I will quiz you about the number afterwards.” can cause failures even in attention-based models, especially on the harder `multikey` tasks. To mitigate this, we apply a light, one-round supervised fine-tuning stage before evaluation to adapt the models to the instruction patterns. We generate 1,000 synthetic training samples for each of the 8 tasks, resulting in a total of 8,000 examples disjoint from the validation sets. The models are trained on this dataset for one round and then are evaluated directly on all 8 tasks. This procedure yields a fairer and more stable comparison. As shown in Table 12, RNNs perform reasonably well on the simpler tasks (`single_1`, `single_2`), but their performance drops to near zero on the harder ones. Attention-based models perform consistently well, benefiting from their ability to access all previous tokens directly. RAT (L=16) achieves results close to full attention, especially in numeric tasks. However, it struggles on UUID tasks due to their complexity and the use of exact match scoring (`single_3`, `multikey_3`). Meanwhile, RAT (L=64) falls between RNNs and RAT (L=16), as expected given its partial access to long-range context.

These results are consistent with the underlying architecture designs: attention provides full direct access to all past tokens, RNNs compress all past information into a hidden state, while RAT compresses part of the history but also retains direct access at the chunk level. As a result, RAT naturally exhibits retrieval capabilities that lie between those of attention and RNNs.

Table 12: Accuracy on the Needle-in-Haystack tasks with different configurations from the RULER benchmark [55], used to evaluate retrieval capabilities. Evaluation is conducted with a 4K context window, using exact match as the metric.

Model	single_1	single_2	single_3	multikey_1	multikey_2	multikey_3	multiquery	multivalue
RNN	99.4	99.8	0.0	2.2	0.0	0.0	5.8	5.7
RAT (L=64)	100.0	99.8	55.6	96.4	62.2	1.0	86.3	89.1
RAT (L=16)	99.6	100.0	94.6	99.6	99.6	82.6	91.2	94.8
Attention	100.0	100.0	100.0	99.6	99.6	95.2	98.6	99.1

D Broader Impacts

Enhancing the efficiency of Large Language Models (LLMs) can significantly reduce computational resources and energy consumption, benefiting the environment and democratizing access to advanced AI technologies. However, increased efficiency could also lead to greater dissemination of disinformation and the creation of deepfakes, posing risks to public trust and security and potentially reinforcing existing biases that impact specific groups unfairly. This research aims to promote the responsible development and deployment of LLMs, maximizing societal benefits while acknowledging potential harms.

E License information

- FineWeb-Edu (dataset): Open Data Commons License Attribution family.
Link: <https://huggingface.co/datasets/HuggingFaceFW/fineweb-edu>
- LongBench (dataset and code): MIT License.
Link: <https://github.com/THUDM/LongBench>

- NarrativeQA (dataset): Apache License 2.0.
Link: <https://github.com/deepmind/narrativeqa>
- QMSum (dataset): MIT License.
Link: <https://github.com/Yale-LILY/QMSum>
- WikiSum (dataset): Custom license (unspecified).
Link: <https://huggingface.co/datasets/d0rj/wikisum>
- lm-evaluation-harness (code): MIT License.
Link: <https://github.com/EleutherAI/lm-evaluation-harness>
- RULER benchmark (code): Apache 2.0 License.
Link: <https://github.com/NVIDIA/RULER>